Experimental Demonstration of the Fermi-Pasta-Ulam Recurrence in a Modulationally Unstable Optical Wave

G. Van Simaeys, Ph. Emplit, and M. Haelterman

Service d'Optique et d'Acoustique, Université Libre de Bruxelles, 50 Avenue F.D. Roosevelt, CP 194/5, B-1050 Brussels, Belgium

(Received 19 March 2001; published 28 June 2001)

Through a detailed spectral analysis of the propagation of square-shaped laser pulses in optical fibers, we provide the experimental demonstration of the Fermi-Pasta-Ulam recurrence phenomenon in modulationally unstable optical waves ruled by the nonlinear Schrödinger equation.

DOI: 10.1103/PhysRevLett.87.033902 PACS numbers: 42.65.Sf, 05.45.Yv, 42.65.Tg, 42.81.Dp

Modulational instability (MI) is a fundamental and ubiquitous nonlinear phenomenon that pertains to a large variety of subfields of physics such as solid-state physics, fluid dynamics, plasma physics, and nonlinear optics. It refers to a process in which a nonlinear and dispersive continuous wave breaks up into a periodic train of localized wave packets. This process is conveniently interpreted in the spectral domain as resulting from energy transfers between the fundamental mode that constitutes the initial continuous wave and higher-order Fourier modes. In the early 1950s Fermi, Pasta, and Ulam (FPU) numerically studied this type of energy transfer between spectral modes in the general context of nonlinear discrete systems [1]. The scope of their investigation was to study the long-term behavior of a chain of coupled nonlinear oscillators initially excited in its fundamental Fourier mode. They initially expected that the nonlinear coupling between the modes would lead to an equipartition of energy between them. However, they observed in their numerical simulations that, instead of leading to the "thermalization" of the system, the energy transfer process involves only a few modes and is reversible in the sense that after a sufficiently long time the system nearly goes back to its initial state.

The discovery of this unexpected behavior, which is now known as the FPU recurrence phenomenon, had a deep impact on the development of modern nonlinear science because it revealed that, contrary to prevalent beliefs, thermalization is not a universal scenario in nonlinear systems. In particular, it led a decade later to the formulation of the soliton concept by Zabusky and Kruskal in the study of the Korteweg–de Vries (KdV) equation resulting from a continuum approximation of the FPU nonlinear lattice problem [2].

Since then, many nonlinear wave equations relevant to a large variety of physical contexts were shown to exhibit FPU recurrence. Among these models, the nonlinear Schrödinger (NLS) equation plays a central role because of its ubiquity in almost all branches of physics. In the context of hydrodynamics, Benjamin and Feir [3] have shown, through a linear stability analysis of deep water waves, that the NLS equation exhibits MI. The study of the dynamical properties of NLS-MI was subsequently performed by means of a truncated three-mode Fourier expansion technique [4]. Although this technique accounts only for the interaction between the initial mode and the two first symmetric sideband modes of the modulated wave, it predicts FPU recurrence for the long-term behavior of MI. The theory of FPU recurrence in the NLS equation was completed and closed afterwards by Akhmediev *et al.* [5] who derived exact analytical periodic solutions that represent the evolution of initially continuous waves.

In contrast with the large number of theoretical studies, experimental demonstrations of FPU recurrence are very rare. This situation is due to the difficulties encountered in practice to maintain the model equations valid over the long durations that characterize the recurrence dynamics. One of the major problems is that FPU recurrence is predicted in conservative systems while any practical system exhibits dissipation. Another issue is the perturbative role played by cumulative higher-order nonlinear effects that are neglected in the theoretical models. As a result, FPU recurrence has been experimentally demonstrated only in very few systems [6]. Demonstrations were performed in electrical networks and in plasmas for the KdV equation, while for the NLS equation FPU recurrence was only observed a little more than 20 years ago in the field of hydrodynamics [7] despite the universality of this generic model in physics. Nonetheless, as regards the practical issue of the long-term validity of the NLS model, nonlinear optics appears to be a promising field of investigation of the FPU recurrence phenomenon because of the availability of low-loss silica optical fibers in which light propagation is accurately ruled by the NLS equation over long distances. Our aim in the present Letter is to show that FPU recurrence of the NLS equation can indeed be demonstrated experimentally in a remarkably convincing way in silica optical fibers.

Although the low-loss and pure Kerr nonlinearity of silica have led to numerous experimental studies of MI in fibers [8], FPU recurrence has never been demonstrated in optics up to now. The reason for this failure is the existence of competing nonlinear effects that invalidate the NLS model over long distances. The Brillouin scattering, which is the most detrimental of these effects, is simply avoided in practice by studying MI in laser pulses instead of continuous wave (cw) signals. Provided the pulse spectrum

is broader than the Brillouin scattering bandwidth, the intensity threshold for this effect can be increased above the pulse intensity. Though this solution is well adapted to the study of MI in the first stage of its evolution [8], the spectral complexity inherent to the pulse profile prevents us from studying FPU recurrence. Indeed, as we shall see, FPU recurrence involves a delicate balance in the energy transfers between a significant number of spectral modes and thus requires spectral purity. To understand this, let us point out that the gain and the characteristic frequency of MI are both strongly dependent on the intensity of light. In a Gaussian-like laser pulse, there is a continuous distribution of intensity levels that is thus associated with different MI gains and frequencies, which unavoidably leads to spectral complexity and destroys the FPU process, as shown in Fig. 1.

In order to overcome this difficulty, we considered for our experiment the use of large square-shaped laser pulses. The large plateau (~550 ps) of these pulses makes them truly quasi-cw signals in the sense that the effects of the rising and trailing edges (~100 ps) are negligible, contrary to what happens in Gaussian-like pulses. In this way, it is possible to observe FPU recurrence that is predicted for pure cw signals. This is illustrated in Fig. 1 where we compare the evolution of a Gaussian pulse and a square pulse of identical full width at half maximum (FWHM). These simulations are obtained by solving numerically the NLS equation with realistic coefficients corresponding to the standard telecommunication silica fiber chosen for our experiment

$$\frac{\partial E}{\partial z} = -i/2\beta_2 \frac{\partial^2 E}{\partial t^2} + i\gamma|E|^2 E\,, \qquad (1)$$

where E is the electric field envelope, z is the propagation distance, t is the time in a reference frame traveling at the group velocity of light, $\beta_2 \approx -21\ \mathrm{ps^2\,km^{-1}}$ is the dispersion coefficient, and $\gamma = 2\pi n_2/\lambda A_{\mathrm{eff}} \approx 1.4\ \mathrm{W^{-1}\,km^{-1}}$ is the nonlinear coefficient, where $\lambda = 1551$ nm is the wavelength of light, $A_{\mathrm{eff}} \sim 87\ \mu\mathrm{m}^2$ is the effective core area of the fiber, and $n_2 = 3.05 \times 10^{-20}\ \mathrm{m^2\,W^{-1}}$ is the nonlinear index coefficient.

We plotted in Fig. 1 the envelopes of both types of pulse at 0.5, 1, and 1.5 recurrence period. As can be seen, recurrence occurs over almost all the plateau of the square pulse while complex nonrecurrent dynamics develop across the entire Gaussian pulse width. This property of the square-shaped pulse is rather general and occurs as long as its rise and fall times as well as the MI period are sufficiently shorter than its plateau. We can thus conclude that the use of square pulses ensures an effective cw regime that allows us to demonstrate the theoretical predictions drawn from the NLS equation with cw initial conditions.

The square pulses that constitute the keystone of our experimental demonstration of FPU recurrence are generated by means of the nonlinear optical fiber loop mirror (NOLM) [9] sketched in Fig. 2. The NOLM is nothing but an all-fiber Sagnac interferometer, which consists of a fiber loop closed on the two output ports of a balanced (50:50) fiber coupler. When a cw signal is launched in the loop through one of the input ports of the coupler (called the NOLM input port), it is entirely reflected back through that port. Partial transmission through the other input port of the coupler (i.e., the NOLM output port) can, however, be obtained if we break the symmetry between the clockwise and counterclockwise optical paths in the loop. This is done in our experiment by injecting an intense control pulse of different wavelength in the loop. The control pulse copropagates in the loop with the clockwise cw signal that, through cross-phase modulation, accumulates locally an additional phase shift along the fiber loop. On the other hand, the nonlinear phase shift imparted on the counterclockwise cw signal remains negligible since it counterpropagates with the control pulse. The clockwise cw signal acquires a nonlinear phase shift over the portion of its envelope that has been superimposed with the control pulse. This portion is determined by the walk-off time accumulated between the signal and the control pulse along the loop due to their group velocity difference. In our experiment the NOLM-input low-power cw signal (~8 mW) is emitted by a distributed feedback semiconductor laser tuned to 1551 nm, while the high-power control pulses are emitted at 1064 nm with a FWHM of 120 ps by a mode-locked Nd:YAG laser. The loop length is of 360 m,

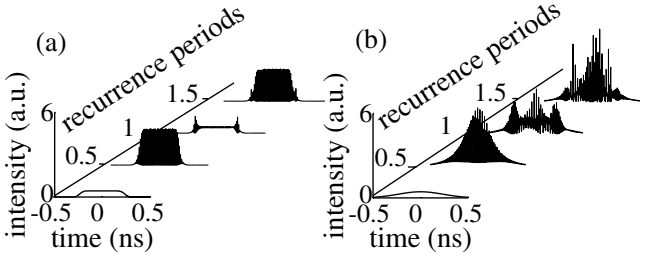

FIG. 1. Envelope evolution over 1.5 recurrence period of (a) a square pulse and (b) a Gaussian pulse with equal initial peak power (2.3 W) and duration (~550 ps).

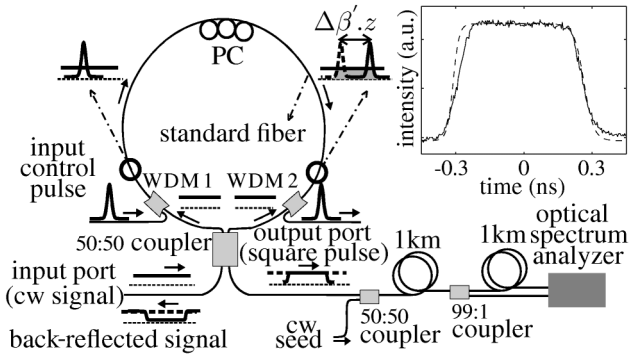

FIG. 2. Experimental setup: square-pulse generator and fiber line. Inset: measured output square-pulse profile (solid line) and profile obtained after deconvolution (dashed line).

which yields a walk-off time of 540 ps corresponding to a standard fiber dispersion. This time represents the duration of the signal transmitted by the NOLM. Maximum transmitted intensity is obtained when the nonlinear phase shift reaches the value of π. We verified experimentally that the peak power of the control pulse corresponding to this situation is of 17 W. The transmitted square pulses were measured with a fast photodiode (response time of ~70 ps) and displayed on a 50-GHz-sampling oscilloscope. The inset in Fig. 2 shows the measured square-pulse profile as well as the profile obtained after deconvolution with the impulse response of the photodiode.

Once the square pulses are generated from the NOLM, they are amplified through an erbium-doped fiber amplifier. The output power of the pulse plateau is tuned between 1 and 2.3 W. MI is seeded by the beating with a small cw signal emitted by a wavelength-tunable source with a power ~30 dB less than the power of the square pulses. The square pump pulses are launched in a 2-km-long standard telecommunication fiber together with the seed signal. We first studied MI dynamics through the simultaneous measurements of the optical spectra at half the fiber length (1 km) and at the fiber output (2 km). The spectra at 1 km are obtained by means of a 1:99 fiber coupler.

Before presenting our experimental results, it is convenient to briefly recall the theory of MI in the NLS Eq. (1). Considering in Eq. (1) an initially perturbed cw of the form $E(t,z) = [\sqrt{P_0} + a(t,z)]\exp(i\gamma P_0 z)$ with $|a|^2 \ll P_0$ and linearizing with respect to a, one gets the following dispersion relation $\kappa = \pm 1/2|\beta_2|\Omega\sqrt{-\Omega^2 - \mathrm{sgn}(\beta_2)\Omega_c^2}$, where κ and Ω, respectively, are the gain and frequency of MI, as defined by $a(t,z) \propto \exp(\kappa z)\cos(\Omega t)$. This expression shows that MI occurs only in the anomalous dispersion regime ($\beta_2 < 0$) and that the MI gain exhibits a finite spectral bandwidth bounded by $\Omega_c = \sqrt{4\gamma P_0/|\beta_2|}$ and with a maximum of $\kappa = \gamma P_0$ located in $\Omega_{\mathrm{opt}} = \Omega_c/\sqrt{2}$. In our experiment, besides the power P_0 (i.e., the power of the square pulses plateau) we control the MI frequency Ω thanks to the seed signal, Ω being merely the frequency detuning of the seed signal with respect to the square pump pulses. In practice, the MI spectral gain profile is directly observed on the optical spectrum analyzer thanks to the amplification of amplifier noise. This allowed us to easily tune the frequency Ω at the optimum MI gain frequency $\Omega = \Omega_{\mathrm{opt}}$ for any value of the input power P_0. The peak power of the square pulses was varied between 1 and 2.3 W. The corresponding range of optimal detuning frequencies Ω_{opt} is 340–520 GHz (0.44–0.66 nm in wavelength).

The spectra at 1 and 2 km were recorded under these conditions for several values of input power P_0. Figures 3(a) and 3(b) show the measured spectra at 1 and 2 km for $P_0 = 2.2$ W. The spectrum exhibits intense sidebands at 1 km and weak sidebands at 2 km, which constitutes a strong indication of the reversibility of the MI process. The graph of Fig. 3(c) shows the evolution of the relative power of the first sideband P_1/P_0 as a function of the pump power P_0 at 1 and 2 km. We see that the relative sideband power at 2 km initially grows with P_0 to reach a maximum in $P_0 \approx 1.5$ W and then goes down to a minimum located in $P_0 \approx 2.2$ W before increasing again. When the sideband power reaches its maximum at 2 km it becomes measurable (i.e., distinguishable from noise) at 1 km. Subsequently, an increase in sideband power is observed at 1 km while it decreases at 2 km, which clearly demonstrates the reversibility of the MI process. In Fig. 3(d) we show together the evolution of the relative powers of the cw component P_{cw}/P_0 and of the first sideband P_1/P_0 at 2 km vs P_0. At $P_0 = 1.55$ W, the maximum of sideband power corresponds to a minimum of cw component power. In solid line, we also show the theoretical curve obtained by numerical simulation of the NLS equation. An excellent agreement between experiment and theory is verified, but it should be noticed that, in order to obtain this agreement, we had to include in our simulation the loss introduced by the 1:99 coupler at 1 km. Although its coupling ratio is rather weak, this coupler has a non-negligible insertion loss (~5%) that affects significantly the MI process. This explains why, contrary to what is predicted with the lossless NLS Eq. (1), the minimum of sideband power at 2 km does not coincide with its maximum at 1 km in Fig. 3(c).

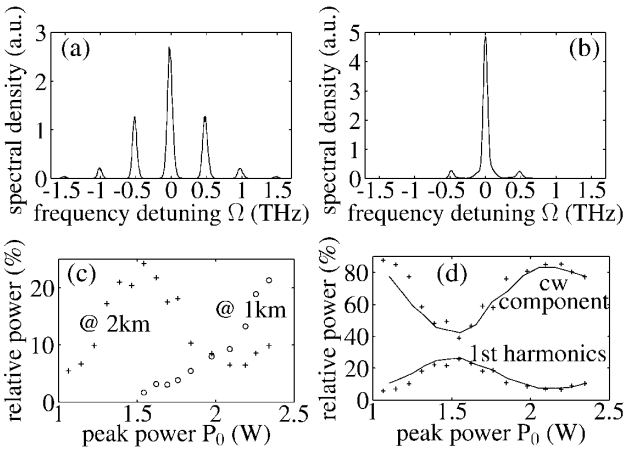

FIG. 3. Square-pulse spectra in linear scale measured at (a) 1 km and (b) 2 km. (c) Relative power of the first sideband P_1/P_0 versus P_0 at 1 km (dots) and 2 km (crosses). (d) Experimental (crosses) and calculated (solid line) relative sideband and pump powers versus P_0 at 2 km.

In order to provide a more complete and accurate analysis of the dynamical features of MI in optical fibers, let us now introduce the following change of variables: $\zeta = \gamma P_0 z$, $\tau = (\gamma P_0/|\beta_2|)^{1/2} t$, and $A = E/(\gamma P_0)^{1/2}$ that transform the NLS Eq. (1) into its canonical form $A_\zeta = i/2\, A_{\tau\tau} + i|A|^2 A$. The evolution in ζ can then be studied at a fixed value of z by simply varying the input power P_0 and we can thus suppress the 1:99 coupler to record the spectra at 2 km without the detrimental effect of insertion loss. With $z = 2$ km, the input power range

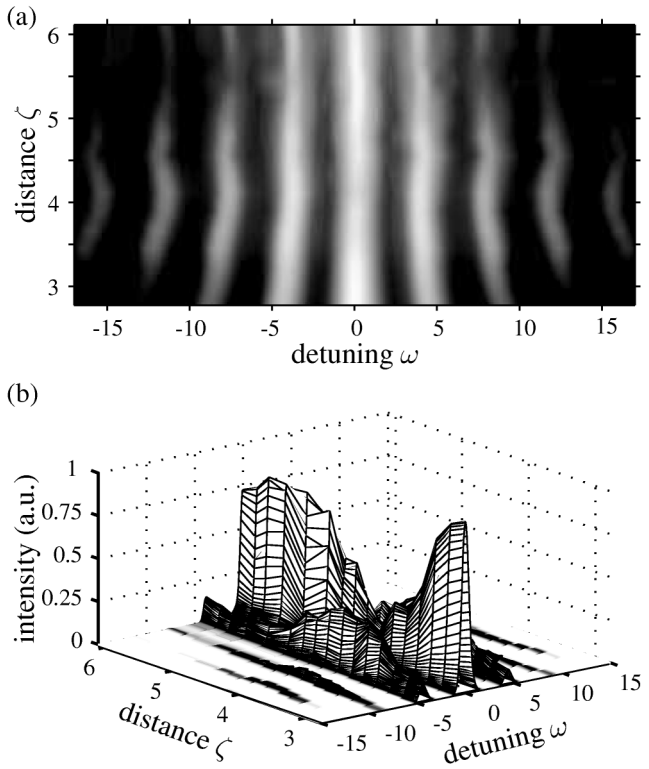

FIG. 4. Recorded MI spectrum evolution. (a) Log scale; (b) linear scale.

1–2.3 W corresponds to a variation of ζ from 2.77 to 6.10, which allows us, as we shall see, to perform a comfortable and detailed study of FPU recurrence.

The experimental results are shown in Fig. 4 that presents the MI spectrum evolution under the form of a density plot in logarithmic power scale and a surface plot in linear power scale [exact scaled units are used on the two other axes, $\zeta = \gamma P_0 z$, $\omega = (\gamma P_0/|\beta_2|)^{-1/2}\Omega$]. We observe that the energy, initially mainly confined in the pump wave ($\omega = 0$), is progressively transferred to the sidebands and their higher harmonics, which leads to a strong pump depletion of approximately 70%, as predicted theoretically [4]. Up to eight detectable modes are involved in this energy exchange process. After a certain propagation distance ($\zeta = 4.1$) the energy transfer is reversed and all the power flows back from the sideband modes to the pump wave. This reciprocal energy exchange process between the pump and a significant number of sideband modes is nothing but the spectral signature of the FPU recurrence phenomenon [1]. The remarkable feature of Fig. 4(a) is that it shows that the power transfer between the sideband modes is perfectly synchronous despite the relatively large number of modes involved. As stated in the theoretical work of Ref. [10], it is this synchronism that allows for a (nearly) return to the initial condition.

In summary, through the study of the propagation of square laser pulses in optical fibers, we have provided the first experimental demonstration of the FPU recurrence phenomenon in modulationally unstable optical waves. Our experiment also constitutes the second demonstration of FPU recurrence in a system ruled by the NLS equation that constitutes a model of fundamental importance in physics. From a practical point of view, our demonstration reveals the validity of the NLS equation for the description of the long-term complex nonlinear behaviors of light waves in silica optical fibers, an issue that is still often the subject of debates. In this sense, the remarkable result of our study is to show that FPU recurrence occurs because the underlying synchronous and reciprocal energy transfer between a significant number of spectral modes is not impaired by perturbations such as linear attenuation and Raman scattering. Our study reveals that the silica optical fiber constitutes an ideal test bed for the experimental investigation of the NLS equation dynamics that are relevant to a large variety of physical systems of both fundamental and applied interests.

This research was supported by the Fonds pour la Formation à la Recherche dans l'Industrie et dans l'Agriculture and by the Inter-University Attraction Pole program of the Belgian government under Grant No. P4-07.

[1] E. Fermi, J. Pasta, and H. C. Ulam, in *Collected Papers of Enrico Fermi,* edited by E. Segrè (The University of Chicago, Chicago, 1965), Vol. 2, pp. 977–988.
[2] N. J. Zabusky and M. D. Kruskal, Phys. Rev. Lett. **15**, 240 (1965).
[3] T. B. Benjamin and J. E. Feir, J. Fluid Mech. **27**, 417 (1967).
[4] P. Henrotay, J. Mec. **20**, 159 (1981); E. Infeld, Phys. Rev. Lett. **47**, 717 (1981); G. Cappellini and S. Trillo, J. Opt. Soc. Am. B **8**, 824 (1991).
[5] N. N. Akhmediev and V. I. Korneev, Theor. Math. Phys. **69**, 1089 (1986).
[6] K. Lonngren, *Soliton in Action,* edited by K. Lonngren and A. Scott (Academic, New York, 1978), pp. 127–152; M. Remoissenet, *Waves Called Solitons* (Springer-Verlag, Berlin, 1994), pp. 67–68.
[7] B. M. Lake, H. C. Yuen, H. Rungaldier, and W. E. Ferguson, J. Fluid Mech. **83**, 49 (1977).
[8] K. Tai, A. Hasegawa, and A. Tomita, Phys. Rev. Lett. **56**, 135 (1986).
[9] N. J. Doran and D. Wood, Opt. Lett. **13**, 56 (1988); K. J. Blow, N. J. Doran, B. K. Nayar, and B. Nelson, Opt. Lett. **15**, 248 (1990).
[10] H. C. Yuen, J. Warren, and E. Ferguson, Phys. Fluids **21**, 1275 (1978).